PAPER REF: 4071

STATIC AND DYNAMIC PROPERTIES OF HYBRID COMPOSITE BEAMS

Jiří Had[1], Milan Růžička[1(*)], Viktor Kulíšek[1], Pavel Steinbauer[1], O. Uher[2]

[1] Department of Mechanics, Biomechanics and Mechatronics, Faculty of Mechanical Engineering, Czech Technical University in Prague, Czech Republic

[2] CompoTech Plus, spol. s r.o., Sušice, Czech Republic

[(*)]*Email:* milan.ruzicka@fs.cvut.cz

ABSTRACT

This work summarizes an evaluation of the static and dynamic properties of hybrid composite beams for the machine tool industry. Special hybrid composite structures were developed, including novel 3D cell structure composite elements, as well as a cork and rubber layer. The requirements on the beam properties for industrial application are introduced. The results of experimental tests (static stiffness, modal properties) are presented, and there is a discussion of the suitability of the simulation tools for predicting these properties.

Keywords: composites, FE models, modal analysis, dynamic stiffness, model validation.

INTRODUCTION

Fundamental properties of machine tools and production systems, e.g. productivity and accuracy, depend significantly on the dynamic properties of their moving parts. These properties can be improved by optimizing the stiffness-over-mass ratio of the current metal components, or by designing new structures using composite materials with high stiffness, low mass and damping. A spindle beam is a highly dynamically loaded machine tool component that can serve as an example of a machine tool application.

The application of fibre composites in the spindle beam can improve the stiffness and damping of the component, and can also improve its thermal stability, due to the low values of the coefficients of thermal expansion of composite materials. The dynamic stiffness/compliance of the machine tool assembly, or more specifically the minimum value of the real part of the dynamic compliance, has a direct influence on the stability of a cutting process, and is directly influenced by the stiffness and the modal damping of the components (Altintas, 2001). The application of lightweight materials can therefore not only reduce the mass of motion axis components, but also improve the cutting stability and in the end increase the machining productivity.

Components of machine tools or production systems are mostly designed to meet high demands on static stiffness; they must meet the conditions on connection interfaces; they are usually in the form of long profiles. Unfortunately, the operating conditions usually require the stiffness of the component to be designed for a combination of different loading modes (bending, torsion, transverse-shearing). For each loading case, stiffness can be achieved by

proper design of the lay-up but, for a combination of loading modes, a change in the structure of the profile may be needed. In that case, the design process is complicated due to the large number of design parameters of 3D composite structures, and sometimes also due to inaccurate behaviour prediction models.

Case studies with various composite profiles were performed in order to provide more knowledge for the design of components. All tested profiles were "beam type" components with different structures, mainly in terms of composite lay-up and material reinforcements. The main goal was to develop a portfolio of composite profiles that would describe the behaviour of the profiles, and would help in selecting the best profile for an application with specified loading conditions and other demands. For each composite profile, the static and dynamic behaviour of the profile was investigated, both experimentally and by numerical simulations. The goal of the work was to compare the properties of the profiles for defined loading cases. The second goal was to evaluate the ability of the numerical models to predict the behaviour of the profile; the accuracy of the prediction was evaluated by comparing it with the experimental results.

COMPOSITE PROFILES

As the basic component, we selected a 1000 mm long beam with a square-like cross-section of dimensions 100x100 mm, see Fig. 1-a. The profile with square-like cross-section with corners reinforced by tubes was derived from the basic profile, see Fig. 1-b. The goal of the tube reinforcements was to provide a possible connection interface, as inserts with threads can be integrated in the tubes. Another profile was created as a hybrid design, combining a square-like composite profile with metal reinforcements, see Fig. 1-c. For comparison, the tube profile was also used, see Fig. 1-d.

a) Simple square beam profile

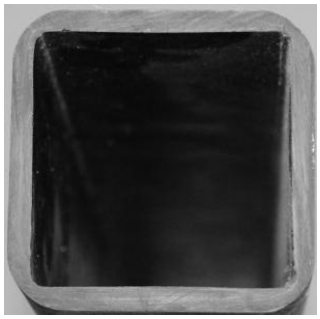

b) Square beam profile with corner reinforcements

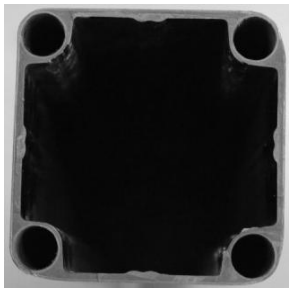

d) Hybrid metal-composite beam profile

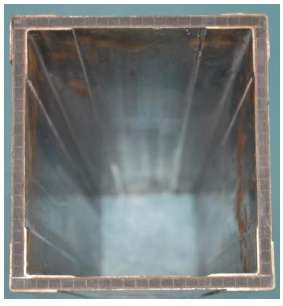

e) Tube beam profile

Fig. 1 Specimens - Beam profiles.

The simple square beam profile was used as the reference specimen to evaluate the properties of all profiles. High-strength (HS) carbon fibres (PAN type) and ultra-high modulus (UHM) carbon fibres (PITCH type) were used as the main reinforcements, combined with anhydride resin. To increase the required parameters, other materials were also used. To increase damping, which should improve the dynamic behaviour, cork layers were used in several variants of the profiles. The integration of cork layers raised the question of improving the damping and reducing the stiffness. Steel reinforcements were used for an investigation of hybrid profiles with enhanced stiffness. The nominal material constants of carbon fibres, epoxy, cork and steel are given in Tab. 1.

Table 1 Nominal constants of the materials in the profiles.

Material	E_L [GPa]	E_T [GPa]	G_{LT} [GPa]	ν_{LT} [-]	ρ [g.mm^{-3}]
High strength fibre (PAN)	235.	15.	50.	0.3	1.80E-03
High modulus fibre (PITCH)	620.	5.	20.	0.35	2.12E-03
Anhydride resin	3.	3.	1.6	0.40	1.13E-03
Damping layer	0.038	0.038	0.008	0.3	8.00E-04
Steel	210.	210.	79.	0.33	7.80E-03

A total of five profiles were compared in the case study:

- a simple square beam profile
- a square beam profile with corner reinforcements
- a square beam profile with corner reinforcements and integrated damping layers
- a tube beam profile with integrated damping layers
- a hybrid metal-composite beam profile with integrated damping layers

A filament winding technology was used for all profiles, except the hybrid metal-composite beam profile. Cork layers for damping were manually integrated to the structures during the winding process. The hybrid metal-composite profile was composed of thin steel skins, cork layers and a three-dimensional cell structure (Růžička, 2009), which was made from cores of uni-directional fibres that were wrapped by a thin C/E layer and pressed together. This structure is mainly used for very thick-walled applications, and it displays very high static stiffness, strength and fatigue life (Had, 2012). A more detailed description of the profiles is given in the section on Profile Analysis.

SETTINGS OF THE EXPERIMENTS

Both an experimental investigation and a numerical investigation of the composite profiles were performed. The goal of the experimental part was to describe the behaviour of the profiles for the defined static loading cases, and to describe the dynamic behaviour of the profiles. Among static properties, stiffness in bending and stiffness in torsion were required. The simulation part was aimed at modelling the experiments and comparing the simulation results (stiffness, eigen-frequencies and mode shapes) with the experimental values.

The specimens were not designed according to any defined standard. The torsion test was therefore performed using an in-house designed torsion fixture. The dynamic behaviour was tested using experimental modal analysis. The goal of the analysis was to determine the mode shapes and the corresponding eigenfrequencies and damping of the profiles. A brief description of the experiments is provided in the following sections.

Experimental investigation of the static properties of the profile

The static stiffness of the profiles was measured in four-point bending (4PB) and torsion configuration. During the four-point bending test, the beam was loaded via the IST-PL40N standalone hydraulic actuator, see Fig. 2. During the experiment, the force and deflection of the actuator was measured together with the strain and deflection of the bottom (unloaded) side of the specimen.

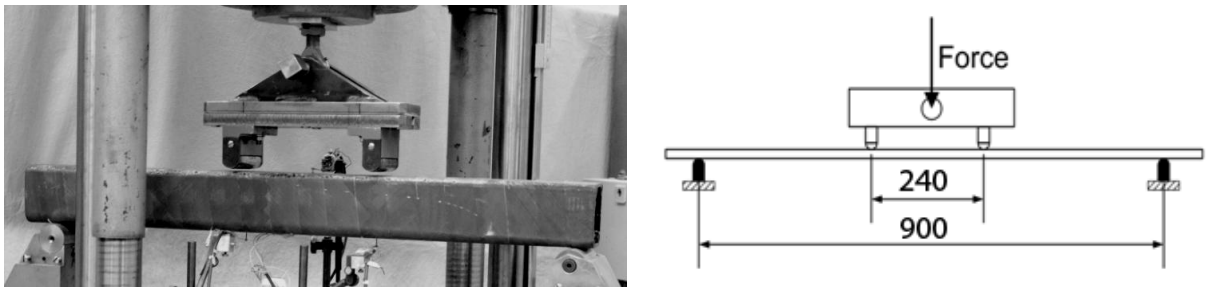

Fig. 2 Four-point bending test configuration

For a comparison of the profiles, bending stiffness EJ was evaluated. The Young's modulus of the profile was determined from the strain gauge (HBM 1-LY11-6/350) between the loading supports; the area moment of the inertia of the cross-section (J) was determined from the geometry of the profile.

The torsion properties were measured using a special torsion fixture, see Fig.3. The specimen was constrained on both sides to prevent additional negative bending, and was loaded with an IST-PL40N actuator with a moment arm of R=176mm.

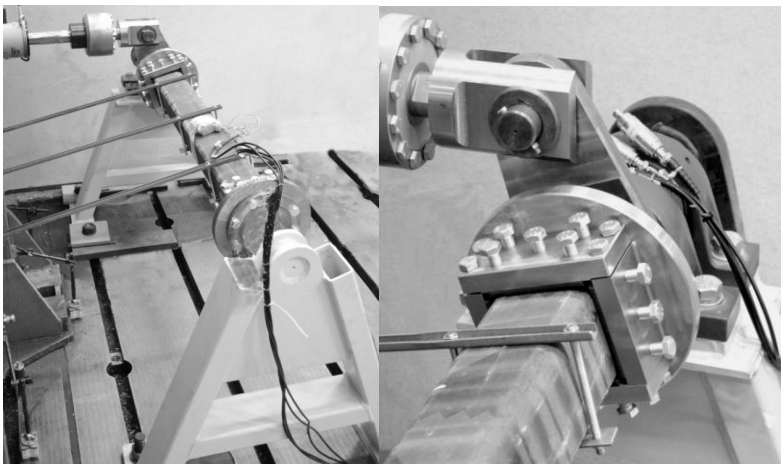

Fig. 3 Organization of the torsion test, and a detail of the torsion fixture

The twisting of the specimen was measured in three planes; the data was used to avoid the influence of the boundary condition. The torsional stiffness GJ_T was determined from the measured moment/final twist ratio, where the final twist was determined as the difference in rotation of the two outer planes.

Experimental investigation of the dynamic properties of the profile

The goal of the experimental modal analysis was to determine the mode shapes, eigen-frequencies and damping of the studied profiles. It was necessary to find the settings and boundary conditions of the experimental modal analysis that have a minimal influence on the evaluated eigen-frequencies and mode shapes. The boundary conditions were achieved by the mounting of the specimens, using low damping/stiffness rubber hooks; these settings had minimal effect on the evaluated properties. The excitation was provided by an electromechanical actuator, which was controlled by a periodic sweep cosine signal. The actuator was connected by a string to the force transducer, which was glued to the tested beam. The string ensured that no additional bending stiffness was introduced into the tested specimen, and that the real acting force in the direction of the string axis was measured by the force transducer.

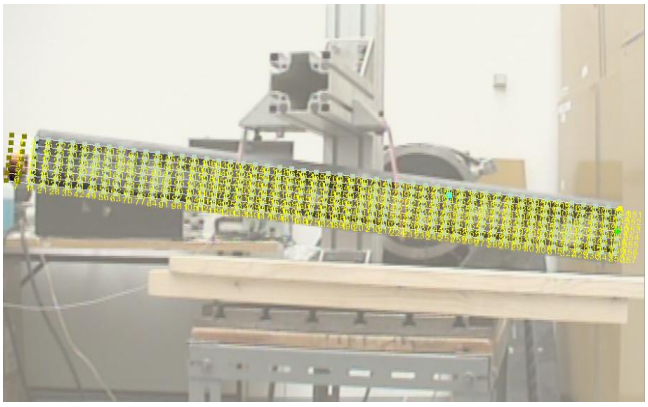

Fig. 4 Set-up for the experimental modal analysis of the specimen

The response signal transducers are another potential source of errors. The roving mass effect of a moving acceleration transducer has been known for many years in experimental modal analysis (Sriram, 1990). Non-contact measurement methods based on laser Doppler vibrometry enable very light and thin structures to be measured (e.g. the measured specimens), without influencing the measured properties. This system was used for an investigation of the properties of the profiles. The laser scanning vibrometer was able to measure a very large number of response points on the test specimen (see Fig. 4). It further improved the accuracy of the results, because the modal properties are global quantities and the data fitting method is based on least squares, where the influence of white noise is reduced with increasing amounts of data. The data fitting method applied here was the Rational Polynomial Fit, which uses the polynomial model of the frequency response function:

$$H(\omega) = \frac{\sum_{k=0}^{N} b_k (j\omega)^k}{\sum_{k=0}^{2*modes} a_k (j\omega)^k}$$

The quality of each measured frequency response function was first evaluated by its coherence function data, and only the best coherence data were used for further processing (see Fig. 5).

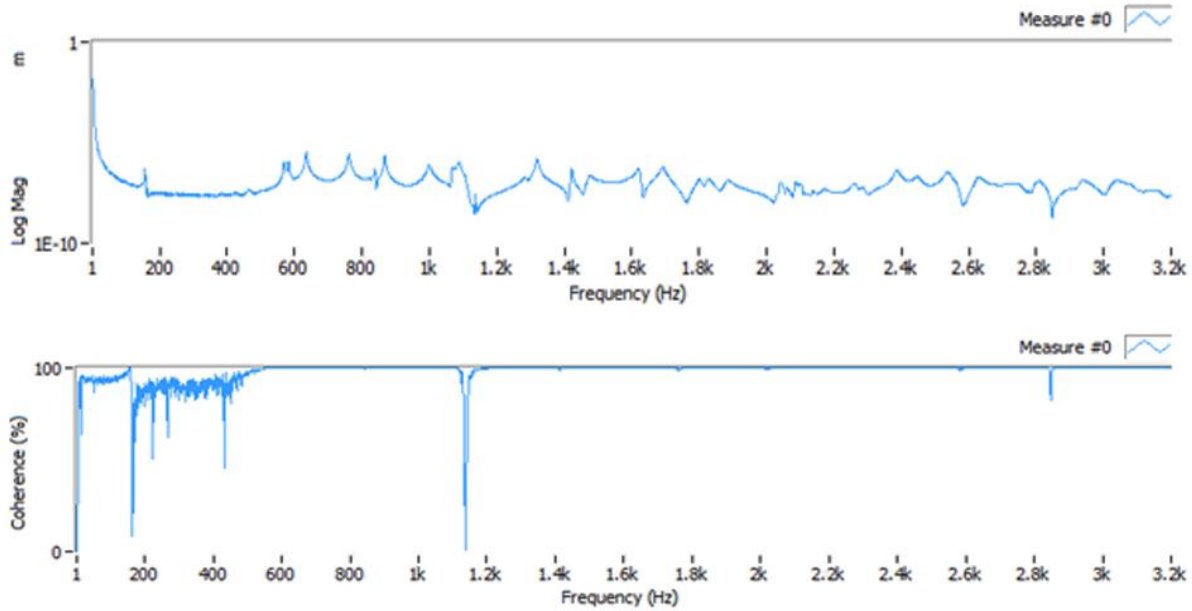

Fig. 5 Example of the amplitude frequency response function and coherence

SETTINGS OF FINITE ELEMENT MODELS

The finite element models of these profiles were prepared for simulations of the four-point bending test, the torsion test and experimental modal analysis. All simulations were performed using the Abaqus standard solver. Conventional or continuum shells were used for modelling the profiles. Brick elements (continuum shells) were necessary, especially for profiles with damping layers, mainly due to the significantly lower stiffness of the damping layers in comparison with the composite layers. The composite lay-up was fully defined to the shell elements, i.e. layer by layer, and the properties of each layer were calculated from the fibres and the matrix properties and the fibre volume fraction, which was determined from the manufacturing technology.

The static experiments were modelled with idealization of the real steel loading fixtures; the idealization was provided by coupling the degrees of freedom (*Kinematic coupling). In the simulations of a four-point bending test, the loading force was distributed on a line of nodes – see Fig. 6; the fixtures were simulated by constraining the translation degree of freedom. For the torsion test, the nodes of each ending were coupled to the central point; the central points were loaded by the torque moment, or were constrained – see Fig. 7. Modal analysis of each profile was performed using free boundary conditions, i.e. no degree of freedom was constrained.

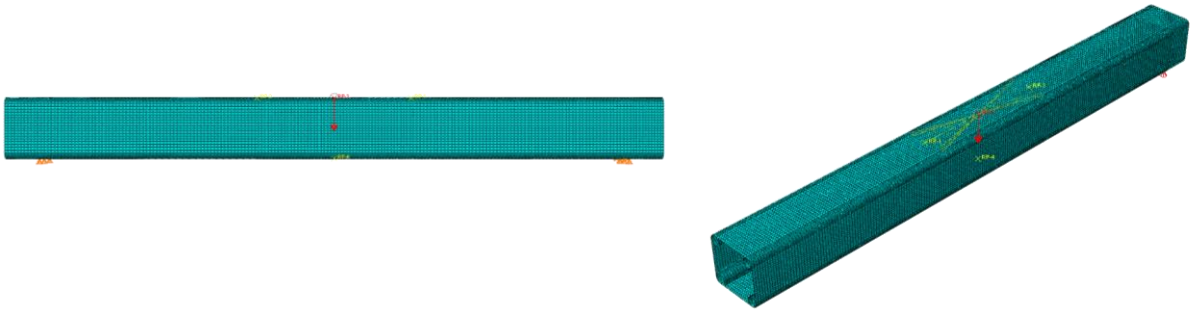

Fig. 6 FE model for prediction of the four-point bending test

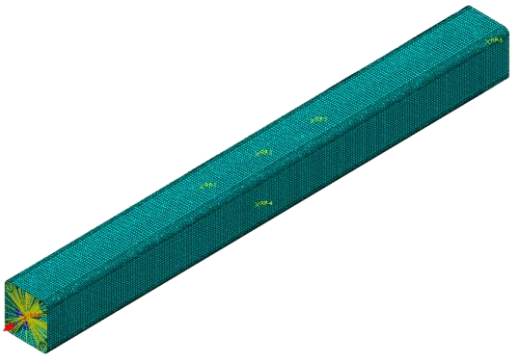

Fig. 7 FE model for prediction of the torque test

PROFILES: COMPARISON OF EXPERIMENTAL AND NUMERICAL RESULTS

This section presents a comparison of the experimental and numerical results. To compare the profiles of different wall thicknesses, or different internal structures, relative stiffness EJ/m and GJ_t/m was selected; where m was the mass of a 1m long specimen. The predicted eigenfrequencies were structural as well as non-structural modes. In the comparison, bending and torsion modes are denoted, as these modes are the most important for applying the profiles.

Simple square beam profile

This specimen was produced from ultra-high modulus fibres only. The beam was made with outer dimensions 100×100mm and nominal wall thickness 8mm. The layup was composed of approximately 70% of 0 degree oriented layers, and the rest was made from ±45 degree oriented layers.

Several numerical approaches were tested (square conventional shell profile; profile with corner idealization by radius), but most of the approaches failed to predict the first eigenfrequencies of the profile. The best results were achieved using a 3D model from continuum shells with non-constant wall thickness in the corners – see Fig. 8

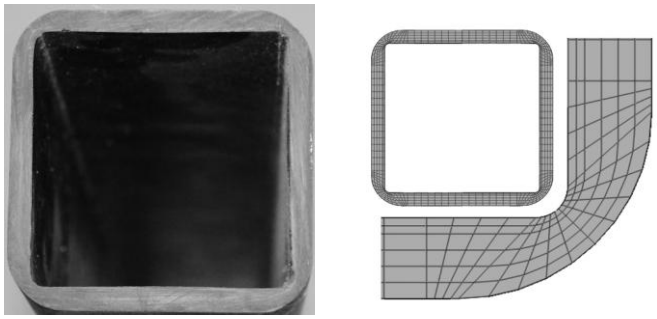

Fig. 8 Simple square beam profile (cross-section - left, FE model – right)

The numerical simulations are compared with the experimental results, see Tab.2. The predicted bending stiffness was 20% higher than the experimentally obtained value; the predicted torsional stiffness was 31% higher than the measured parameter. The presented model predicted the first 5 natural frequencies within 10% of difference from the experimental result.

Table 2 Experimental and numerical results for the square beam profile.

	EJ_x/m	GJ_p/m	f_1	f_2 –torsion	f_3	f_4 - bending	f_5–
	[Nmm^2/kg]	[Nmm^2/kg]	[Hz]	[Hz]	[Hz]	[Hz]	[Hz]
FEM	2.66E+11	3.65E+10	656	695	1401	1495	1432
EXP	2.22E+11	2.79E+10	625	690	1285	1398	1452
ΔFEA/exp	20%	31%	5%	1%	9%	7%	-2%

A simple square beam with tube reinforcements

This specimen was produced both from ultrahigh modulus fibre and from high strength fibre. The outer dimensions were 100×100mm, and the nominal thickness was 3.5mm. More than 55% of the lay-up was designed from UHM fibres with 0 degree orientation; the rest was composed of high-strength fibres with 85 or ±45° degree orientation. The outer diameter of the tubes in the corners is 16mm, and the thickness is 1mm. The tubes are produced only from high-strength fibre. Their lay-up was made from a combination of ±30°and 90° layers. The profile and its FE model are shown in Fig. 9. A shell model was used to model this thin-walled structure. Proper modelling of the corners was found to be a crucial consideration for precise prediction. The tubes were connected tangentially with the sheet, via auxiliary stringers with equivalent thickness,

Fig. 9 Simple square beam profile with tube reinforcements (cross-section - left, FE model – right)

A comparison of the numerical simulations with the experimental results is presented in Tab. 3. The predicted bending stiffness was 20% higher than the experimentally obtained value; the predicted torsional stiffness was 20% lower than the measured parameter. The presented model matched well with the first torsion and bending mode, but other modes, which were dependent on the modelling of the corners, were predicted with high variation between FEA and experiment. A comparison of the numerical simulations and the experimental results is presented in Tab.2. The predicted bending stiffness was 20% higher than the experimentally obtained value; the predicted torsional stiffness was 31% higher than the measured parameter. The model presented here predicted the first 5 natural frequencies within 10% of difference from the experimental result.

Table 3 Experimental and numerical results for the square beam profile with corner reinforcements.

	EJ_x/m	GJ_p/m	f_1	f_2-torsion	f_3	f_4	f_bending
	[Nmm^2/kg]	[Nmm^2/kg]	[Hz]	[Hz]	[Hz]	[Hz]	[Hz]
FEM	1.84E+11	1.39E+10	550	553	722	789	1051
EXP	1.56E+11	1.71E+10	567	583	635	762	1069
ΔFEA/exp	18%	-19%	-3%	-5%	14	4%	-2

Simple square beam with tube reinforcements and damping layers

The specimen was similar to the profile mentioned above; the only difference was in the 2mm thick damping layer that was integrated into the composite lay-up. The profile and an FE model of it are shown in Fig. 10.

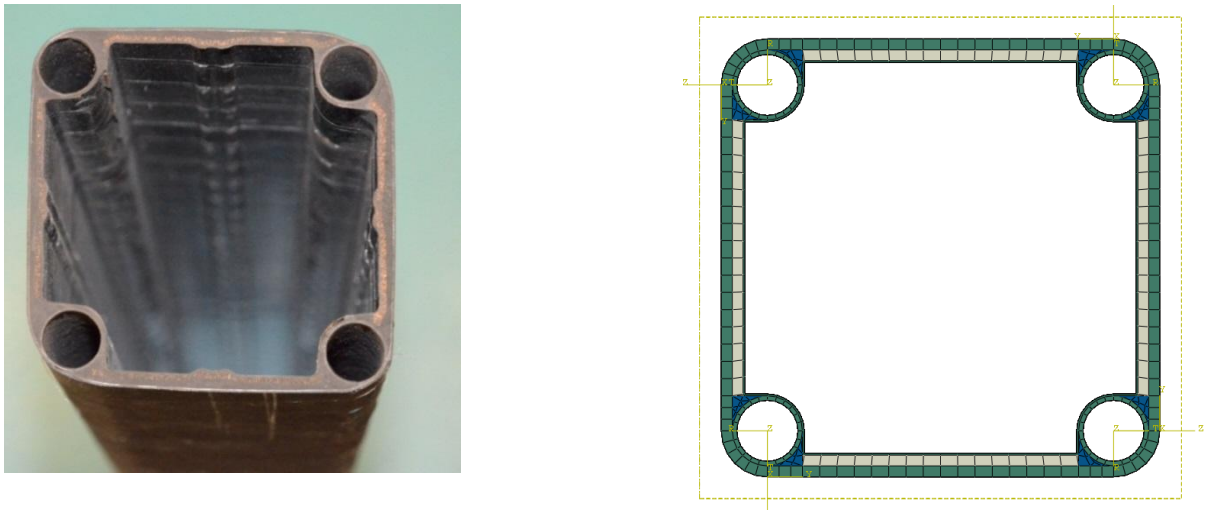

Fig. 10 Simple square beam profile with tube reinforcements and damping layers (cross-section - left, FE model – right)

Although the FE model of the profile with corner reinforcements and a damping layer was modelled with a higher level of detail than the model of the profile without the damping layers, the FEA-to-experiment comparison of this profile showed significantly worse results. The comparison is presented in Tab. 4. The model predicted well the behaviour in the first bending and torsion mode (the difference between FEA and the experimental results was

below 11%). However, the FE model predicted completely different frequencies of the comparable eigen modes of the first 4 mode shapes. The static stiffness was also predicted with significantly higher variation than was predicted by the model of the profile without the damping layers.

Table 4 Experimental and numerical results for the square beam profile with corner reinforcements and damping layers.

	EJ_x/m	GJ_p/m	f_1	f_2-torsion	f_3	f - bending	f - torsion
	[Nmm^2/kg]	[Nmm^2/kg]	[Hz]	[Hz]	[Hz]	[Hz]	[Hz]
FEM	1.69E+11	1.02E+10	864	894	x	954	1046
EXP	1.28E+11	1.64E+10	558	645	738	918	1176
ΔFEA/exp	32%	-38%	55	38	Not identified	4	11

In this case, the accuracy of the model was strongly influenced by the presence of a damping layer, as the material parameters of the layer were significantly lower than the parameters of the fibre composite layers. The damping layers were placed on the straight parts of the profile. The results may have been influenced by inaccuracies of the material constants and by the irregular thickness of the damping layer.

Tube beam profile with integrated damping layers

Another example of a profile with integrated damping layers was the tube beam profile – see Fig. 11. The outer diameter of the profile was 70mm, and the inner diameter was 35mm. 11mm of the overall thickness was made from ultra-high modulus fibres; 2.5 of the thickness was made from high-strength fibres; the rest from damping layers. The lay-up was composed of layers with 0 degree orientation (52%), ±45° degree orientation (40%) and 85 degree orientation (8%).

The profile was modelled using continuum shell elements; this approach was selected as it enabled the damping layers to be modelled with single elements per thickness of the layer. A comparison of the experimental results and the numerical results is presented in Tab. 5.

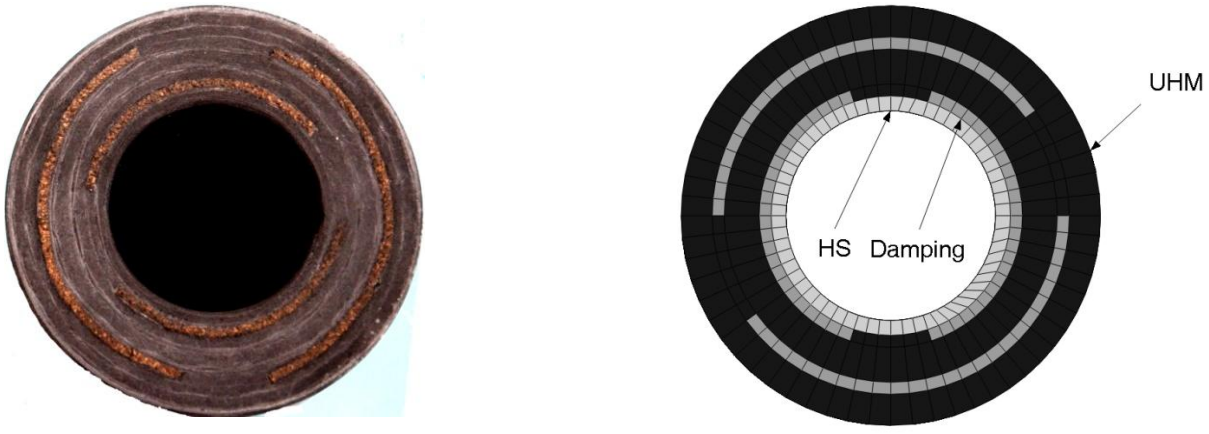

Fig. 11 Tube beam profile

Table 5 Experimental and numerical results for the tube beam profile with damping layers.

	EJ_x/m	GJ_p/m	f1 – bending	f2 – bending	f3 – torsion	f4 - bending
	[Nmm^2/kg]	[Nmm^2/kg]	[Hz]	[Hz]	[Hz]	[Hz]
FEM	5.21E+10	5.30E+7	484	1196	1298	2081
EXP	N/A	N/A	452	1123	1142	1911
Δ	-	-	7%	6%	14%	9%

Although the model was assembled with a similar approach to that used for the beam profile with corner reinforcements and integrated damping layers, in this case it led to acceptable results that were in good agreement with the experiment for bending modes.

Simple square profile with a 3D structure

The hybrid metal-composite design of the square beam profile used various types of material; each component had its own functionality. The beam was produced from 4 sandwich plates and plates that were jointed together in the corners. The sandwich plate consisted of steel skins and a 3D composite core. The damping layers were placed between the skins and the core. The outside dimensions were 160×172mm, and the nominal thickness was 6mm, see Fig. 12.

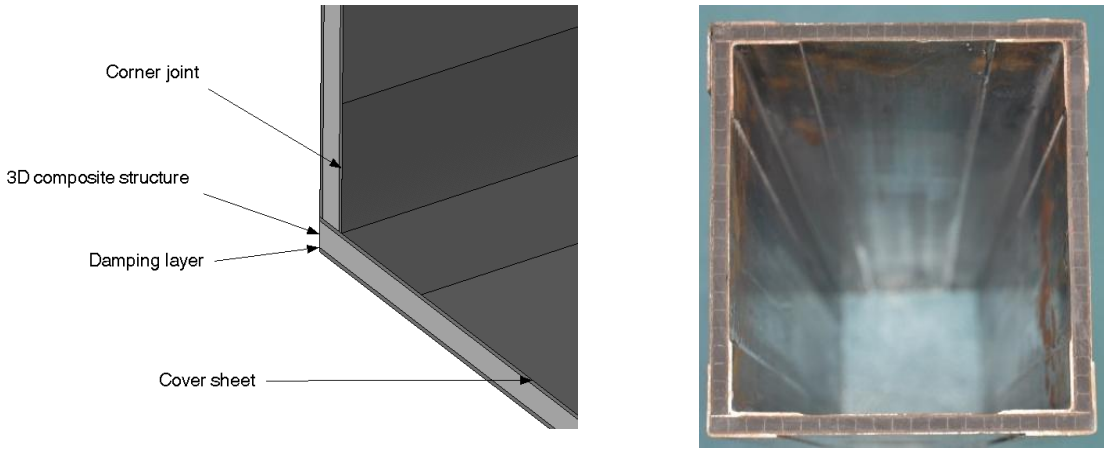

Fig. 12 Hybrid metal-composite beam profile

The model of the profile was made using various approaches for each component of the profile. The steel skins were modelled using conventional shell elements; the damping layers were modelled using solid (brick) elements; the 3D composite structure was modelled with solid elements, using a homogeneous material with equivalent homogenized material data (Růžička, 2011). A comparison of the FEA and experimental results is presented in Tab. 6. A comparison of the predicted and experimentally determined frequencies showed good agreement, with variations below 5%. Due to the geometry of the specimen, most of the presented mode-shapes are non-structural – wall vibrations.

Table 6 Experimental and numerical results for a hybrid metal-composite beam profile.

	EJ_x/m	GJ_p/m	f1	f2	f3	f4
	[Nmm^2/kg]	[Nmm^2/kg]	[Hz]	[Hz]	[Hz]	[Hz]
FEM	5.09E+11	1.66E+10	213.0	496.9	561.0	864.2
EXP	N/A	N/A	225.0	477.0	558.0	855.0
ΔFEA/exp			5%	-4%	-1%	-1%

DISCUSSION

Comparison of the properties f the profiles

A comparison of the profiles is presented in Tab. 7. The bending and torsional stiffness in relation to the unit mass of the specimens were compared, together with the frequency of the first torsion and bending modes. A comparison was also made of the damping of these modes and the averaged damping evaluated from the first 10 modes. Tab. 8 presents the same comparison in relation to the results for the square beam profile.

Table 7 A comparison of the experimentally determined properties of the profiles (* denotes properties from simulations; X denotes a change in the dimensions of the cross-section of the profiles).

Profile	EJ_x/m	GJ_p/m	f-bending	f-torsion	ζ - bending	ζ– torsion	ζ average
	[Nmm^2/kg]	[Nmm^2/kg]	[Hz]	[Hz]	[%]	[%]	[%]
Square	2.22E+11	2.79E+10	1398	690	0.10	0.31	0.31
Square with reinforced corners	1.56E+11	1.71E+10	1069	583	0.21	0.27	0.23
Square with reinforced corners and damping	1.28E+11	1.64E+10	918	645	2.66	2.98	1.79
Tube with damping^X	5.21E+10*	5.30E+7*	452	1142	0.25	0.26	0.59
Square hybrid steel-composite^X	5.09E+11*	1.66E+10*	N/A	N/A	N/A	N/A	N/A

Table 8 A comparison of the experimentally determined properties of the profiles related to the square beam profile(* denotes properties from simulations, X denotes a change in the profile cross-section dimensions).

Profile	EJ_x/m	GJ_p/m	f-bending	f-torsion	ζ - bending	ζ– torsion	ζ average
	[%]	[%]	[%]	[%]	[%]	[%]	[%]
Square	100	100	100	100	100	100	100
Square with reinforced corners	70	61	76	84	210	87	74
Square with reinforced corners and damping	58	59	66	93	2660	961	577
Tube with damping^X	23*	0.19*	32	165	250	84	190
Square hybrid steel-composite^X	229*	59*	N/A	N/A	N/A	N/A	N/A

This comparison needs to be evaluated carefully, as it has been made from profiles of different lay-up and, in the case of the tube and hybrid profile, from profiles with different cross-sectional dimensions.

In terms of static stiffness in bending, the hybrid metal-composite square profile provided results superior to those of the other profiles. The high stiffness resulted from larger profile dimensions and also from the combination of steel and composite layers. The presence of soft damping layers did not significantly reduce the stiffness. The torsion properties were comparable to those of the square beam profile.

The square beam profile was comparable with the profile with reinforced corners, and with the profile with reinforced corners and integrated damping layers. The basic profile had the highest stiffness, as it was made with approximately two times higher wall thickness. The average damping ratio was comparable to the damping ratio of the profile with reinforced corners. A reduction in the stiffness of the profiles with reinforced corners was caused by the smaller wall thickness and also by the lower efficiency of the material in the corners. Integrating the damping layers made from low-stiffness material reduced the stiffness by another 10-12% in the case of bending. In the case of torsion, integrating the transverse shear stiffness had a marginal stiffening effect. However, the average damping of the profile with damping layers was several times higher (5÷8 times) than the average damping ratio of the profiles without the damping layers.

The tube profile was selected to again demonstrate the profile with integrated damping layers. Although the damping of the first bending and torsion mode shapes was comparable with the damping of the square beam profiles without damping layers, the average damping ratio was two times higher. However, this profile with damping layers yielded significantly lower damping than the square beam profile with damping layers. One explanation for this is that the damping layer was not integrated into the whole circumference of the cross-section, but only into two sectors of the cross-section.

Discussion of Finite Element Models

The finite element models of the profile were prepared with a high level of detail in the models, as one of the planned applications was to use the verified models as reference models for developing simplified predictive tools. The models were compared with the experimental values, and for comparison the parameters for static bending and torsional stiffness and the eigen-frequencies of the same mode shapes were used.

The accuracy of the detailed models turned out to be questionable, especially for the static stiffness of the square beam profiles with or without the reinforced corners. The models of the square beam profiles over-predicted the static stiffness in bending by 20% to 30%. However, the frequency of the first bending mode shape was predicted with disagreement to experiment below 10%. There was larger disagreement between the experiment and the FE model when predicting the behaviour in torsion. The stiffness in torsion was over-predicted or under-predicted; the results differed for each profile. Again, the torsional eigen-frequencies were predicted with better accuracy than the static stiffness. The high disagreement between the FEA and the experimental results for static stiffness may have been caused by the idealized modelling of the experimental boundary conditions, as the agreement in the bending and torsional eigen-frequencies was significantly higher.

In the case of modal analysis, there was an acceptable level of agreement (below 10%); further improvement of the models can be achieved by more precise definition of the material parameters of the lay-up layers, which were made by the filament winding technology.

The study showed that the modelling of the corners of profiles is crucial to achieve good accuracy for the complete spectrum of the mode shapes. Modelling the square beam profile

with damping layers was particularly problematic. For this profile, a combination of manufacturing irregularities, the presence of soft damping layers, and the complicated structure introduced many questionable parameters that resulted in the final inaccuracy of the model. For the tube model with damping layers from the same material, very good agreement between the FE simulations and the experimental values was achieved.

CONCLUSIONS

The study presented here was used to evaluate the static and dynamic properties of composite or hybrid metal-composite beam profiles. The focus was on the stiffness in bending and torsion loading modes, and on eigen-frequencies and damping. Conclusions were derived on the changes in static stiffness and damping when the soft damping layers are integrated in the lay-up. Integrating the damping layers led to an approximately 18% reduction in bending stiffness and a 4% reduction in torsional stiffness, while the average damping ratio was stiffened almost eightfold.

ACKNOWLEDGMENTS

The authors would like to thank the Ministry of Industry and Trade of the Czech Republic for supporting this research in the framework of project no. TA02010543. Support from the CompoTech Plus Company in manufacturing the composite specimens is also gratefully acknowledged.

REFERENCES

Altintas Y., Engin S. Generalized Modeling of Mechanics and Dynamics of Milling Cutters. CIRP Annals, Manufacturing Technology, Volume 50, Issue 1, 2001, p. 25–30

Had J. Růžička M. Fatigue Properties of the Cell 3D Composite Structure by Tension and Shear. Proceedings of the ECCM15, Venice, Italy, 24-28 June 2012.

Růžička M., Kulíšek V., Had J., Prejzek O. Determination of Elastic Constants of Novel Concept 3D Composite. Bulletin of Applied Mechanics. 2009, vol. 5, no. 20, p. 87-92. ISSN 1801-1217.

Růžička, M., Had J., Kulíšek V., Uher O. Multiscale Modeling of Hybrid Composite Structures. Key Engineering Materials Vols. 471-472 (2011) pp 916-921.

Sriram P., Craig J. I.; Hanagud S. A scanning laser Doppler vibrometer for modal testing. International Journal of Analytical and Experimental Modal Analysis (ISSN 0886-9367), vol. 5, July 1990, p. 155-167.